Ultrafast electron-phonon interaction of intersubband transitions: Quantum kinetics from adiabatic following to Rabi-oscillations

Stefan Butscher,* Jens Förstner, Inès Waldmüller, and Andreas Knorr
Institute for Theoretical Physics, Nonlinear Optics and Quantum Electronics, Hardenbergstrasse 36 PN 7-1, 10623 Berlin, Germany
(Received 15 February 2005; revised manuscript received 11 May 2005; published 8 July 2005)

The interaction of electrons with LO phonons provides an important mechanism of optical dephasing and carrier scattering for the two-dimensional electron gas in semiconductor quantum wells. In this paper, the corresponding ultrafast nonlinearities for off-resonant and resonant intersubband excitations are investigated. Quantum kinetic effects of the electron-phonon interaction and the corresponding violation of the microscopic energy conservation yield a qualitative different picture compared to the standard Markovian theory, if the phonon energy is larger than the intersubband-gap energy.

DOI: 10.1103/PhysRevB.72.045314 PACS number(s): 42.50.Md, 71.38.−k, 78.67.De

In ultrafast optics, a two-level system is a well-known model system for nonlinear effects ranging from an instantaneous response of the induced dipole to the shape of the light pulse (adiabatic following or Kerr nonlinearity) for off-resonant excitation to saturation effects (Pauli blocking) and Rabi flopping for resonant excitation.[1] Similar effects can also be observed for transitions between two bands in semiconductors.[2] However, compared to an atomic system such coherent optical nonlinearities in a semiconductor can be modified or completely suppressed by many-body effects, such as electron-phonon (el.-ph.) and electron-electron interaction.[3–5] For example, modified Rabi oscillations have been observed in semiconductor bulk material[6,7] as well as in semiconductor nanostructures, like quantum dots[8,9] and quantum wells.[10] Recently, experimental progress in the infrared and terahertz (THz) regime allows the extension of these studies to intersubband (ISB) transitions in a two-dimensional electron gas in a semiconductor quantum well (QW).[11,12] More experimental observations of ultrafast optical nonlinearities in this low energy regime are expected to be published in the near future.

In this paper, we aim at the importance of the quantum kinetics of the el.-ph. interarction for ISB nonlinearities and evaluate a theory of the optically induced ISB response in a deep semiconductor QW. The analysis includes the energetically lowest two subbands. Due to doping the subbands are populated with a two-dimensional electron gas forming a Fermi-distribution in the ground state, compare. Fig. 1. The optical field can be used to induce ISB transitions between both subbands (solid arrow). Material parameters, such as the subband energy $\varepsilon(\mathbf{k})$ were taken from a GaAs/AlGaAs QW. Nonparabolicity effects of the conduction band lead to different effective masses of each subband.[13] The masses can be calculated according to Ref. 16. As a first approach to many-particle scattering and dephasing mechanisms for ISB transitions in nonlinear optics we discuss the coupling of the electronic system to a bath of optical bulk phonons, which are not confined by the QW, on a quantum kinetic (non-Markovian) and on a semiclassical (Markovian) level. Such a treatment of the phonons has already been used for quantum dots.[14,15] Quantum kinetic (el.-ph.) scattering was found to be important for ultrafast nonlinear optical excitations in bulk material and nanostructures.[17,18] Measurements of the nonlinear absorption of GaN/AlGaN QWs indicate a prominent role of quantum kinetics of the el.-ph. interarction.[19] Theoretical investigations are so far restricted to a detailed analysis of the linear optical properties (line shape) (Refs. 20 and 21) and their quantum kinetics.[22]

The model system is described by the Hamiltonian $H=H_0+H_{\mathrm{el,ph}}+H_{\mathrm{dip}}$, where H_0 describes the free kinetics of the electrons and phonons, $H_{\mathrm{el,ph}}$ the el.-ph. interaction and H_{dip} the electron-light dipole interaction.[20] H_0 reads

$$H_0=\sum_{i,\mathbf{k}}\varepsilon_{i\mathbf{k}}a_{i\mathbf{k}}^{\dagger}a_{i\mathbf{k}}+\sum_{\mathbf{q}}\hbar\omega_{\mathrm{LO}}b_{\mathbf{q}}^{\dagger}b_{\mathbf{q}}. \tag{1}$$

Here, $\varepsilon_{i\mathbf{k}}=\hbar^2\mathbf{k}^2/2m_i+\varepsilon_{\mathrm{gap}}$ is a single particle energy of an electron in subband i with an in-plane wave-vector $\mathbf{k}$ and $\hbar\omega_{\mathrm{LO}}$ is the phonon energy (36 meV), while $a_{i\mathbf{k}}^{\dagger}$, $a_{i\mathbf{k}}$, and $b_{\mathbf{q}}^{\dagger}$, $b_{\mathbf{q}}$ are creation and annihilation operators for the electrons in the subbands $i=1$, 2 with $2d$ wave-vector $\mathbf{k}$ and phonons with the $3d$ wave-vector $\mathbf{q}$. The Hamiltonian of the el.-ph. interarction is given by

$$H_{\mathrm{el,ph}}=\sum_{i,j,\mathbf{k},\mathbf{q}}(g_{\mathbf{q}}^{ij}a_{i,\mathbf{k}}^{\dagger}b_{\mathbf{q}}a_{j,\mathbf{k}-\mathbf{q}_{\parallel}}+g_{\mathbf{q}}^{ij*}a_{j,\mathbf{k}-\mathbf{q}_{\parallel}}^{\dagger}b_{\mathbf{q}}^{\dagger}a_{i,\mathbf{k}}). \tag{2}$$

Here, $\mathbf{q}_{\parallel}$ denotes the in-plane projection of the phonon wave-vector $\mathbf{q}$ and $g_{\mathbf{q}}^{ij}$ are the Fröhlich coupling matrix

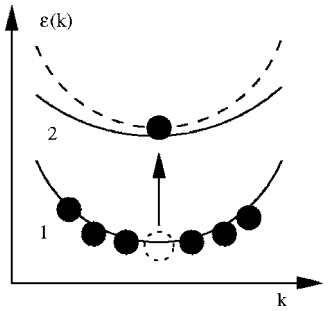

FIG. 1. Schematic diagram of the band structure of a two-band system with different subband masses (solid line) and equal subband masses (dashed line).

elements.[20,21] The dipole interarction of the electrons with a classical electric field reads

$$H_{\mathrm{dip}} = \sum_{i,j,\mathbf{k}} M_{ij} E(t) a^{\dagger}_{i,\mathbf{k}} a_{j,\mathbf{k}}. \tag{3}$$

Here, $E(t)$ is the z component of the external electric field at the QW position and M_{ij} are the dipole matrix elements.[20,21] The Heisenberg equations for the electron occupations $f_{ii,\mathbf{k}} = \langle a^{\dagger}_{i\mathbf{k}} a_{i\mathbf{k}} \rangle$ in subbands i at the wave-vector $\mathbf{k}$ and the ISB coherences (microscopic polarization) $f_{ij,\mathbf{k}} = \langle a^{\dagger}_{i\mathbf{k}} a_{j\mathbf{k}} \rangle (i \neq j)$ at wave-vektor $\mathbf{k}$ are

$$\frac{d}{dt} f_{ij,\mathbf{k}} = -i\omega_{i\mathbf{k},j\mathbf{k}} f_{ij,\mathbf{k}} + \frac{iE(t)}{\hbar} \sum_{l} (M_{jl} f_{il,\mathbf{k}} - M_{li} f_{lj,\mathbf{k}}) - \frac{1}{i\hbar} \sum_{l,\mathbf{q}} [g^{li}_{\mathbf{q}} s^{lj}_{\mathbf{k}+\mathbf{q}_{\parallel},\mathbf{q},\mathbf{k}} + g^{il}_{\mathbf{q}} s^{lj*}_{\mathbf{k}-\mathbf{q}_{\parallel},\mathbf{q},\mathbf{k}} - g^{jl}_{\mathbf{q}} s^{il}_{\mathbf{k},\mathbf{q},\mathbf{k}-\mathbf{q}_{\parallel}} - g^{lj}_{\mathbf{q}} s^{il}_{\mathbf{k},\mathbf{q},\mathbf{k}+\mathbf{q}_{\parallel}}]. \tag{4}$$

Here, we have introduced $\omega_{i\mathbf{k},j\mathbf{k}} = (\varepsilon_{i,\mathbf{k}} - \varepsilon_{j,\mathbf{k}})/\hbar$ and the phonon-assisted density matrix elements (PDM) $s^{ij}_{\mathbf{k}+\mathbf{q}_{\parallel},\mathbf{q},\mathbf{k}} = \langle a^{\dagger}_{i\mathbf{k}+\mathbf{q}_{\parallel}} b_{\mathbf{q}} a_{j\mathbf{k}} \rangle$.[23] In order to obtain a closed set of equations we have performed a correlation expansion[24,25] up to second order in $g^{ij}_{\mathbf{q}}$ (single phonon process). This yields

$$\frac{d}{dt} s^{ij}_{\mathbf{k}+\mathbf{q}_{\parallel},\mathbf{q},\mathbf{k}} = i(\omega_{i\mathbf{k},j\mathbf{k}+\mathbf{q}_{\parallel}} - \omega_{LO}) s^{ij}_{\mathbf{k}+\mathbf{q}_{\parallel},\mathbf{q},\mathbf{k}} - \frac{i}{\hbar} \sum_{lm} g^{ml*} \times [(n_{\mathbf{q}} + 1) f_{im,\mathbf{k}+\mathbf{q}_{\parallel}} (\delta_{lj} - f_{lj,\mathbf{k}}) - n_{\mathbf{q}} f_{lj,\mathbf{k}} (\delta_{im} - f_{im,\mathbf{k}+\mathbf{q}_{\parallel}})] - \gamma_{ph} s^{ij}_{\mathbf{k}+\mathbf{q}_{\parallel},\mathbf{q},\mathbf{k}}. \tag{5}$$

Here, $n_{\mathbf{q}}$ denotes the Bose-Einstein distribution for the phonons, determined by the lattice temperature T and the phonon energy. The Markov approximation of Eq. (5) is discussed in Refs. 22 and 24; instead of the differential equation Eq. (5) one gets an explicit expression for $s^{ij}_{\mathbf{k}+\mathbf{q}_{\parallel},\mathbf{q},\mathbf{k}}$, that is only depending on the single-particle quantities such as $f_{ij,\mathbf{k}}$. In Eq. (5) we have introduced the phenomenlogical damping constant γ_{ph}, which was found to enhance numerical stability, without changing our results or their interpretation, as long as γ_{ph} is smaller than the el.-ph. interaction induced linewidth of the linear absorption spectra.[22] We have verified that in the nonlinear regime, the choice of γ_s has no impact onto results, as long as $\hbar\gamma_{\mathrm{ph}} \leqslant 1$ meV [cp. Fig. 3(b)]. If not mentioned otherwise, we use $\hbar\gamma_{\mathrm{ph}} = 1$ meV.

In the following the quantum kinetic equations, Eqs. (4) and (5), are evaluated numerically. In contrast to Ref. 22, which focused on linear absorption, this paper analyzes the nonlinear ultrafast optical response which in the time domain for the quantum kinetic and the Markovian regime. We start by investigating resonant excitation (1) where we expect Rabi flopping of the carrier density for sufficiently short and strong pulses and subsequently focus on well off-resonant excitations (2), dominated by adiabatic following which corresponds to a Kerr nonlinearity. Furthermore, we demonstrate that the Markovian approach fails for gap energies smaller than the phonon energy (3).

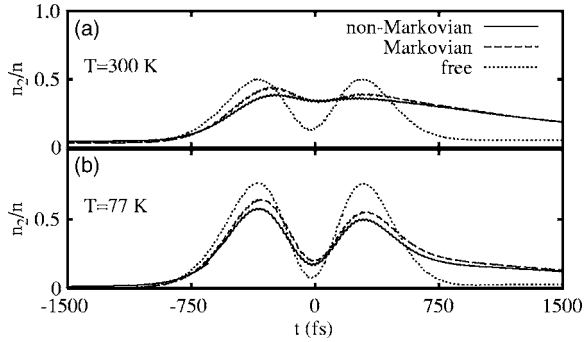

FIG. 2. Relative population n_2/n of the upper subband in a 10 nm wide QW that has a carrier density of $n = 6.0 \times 10^{11}$ cm^{-2} with non-Markovian (solid line), Markovian (dashed line) el.-ph. interarction, and for free carriers (dotted line) at a lattice temperature (a) $T = 300$ K and (b) 77 K.

In all three cases, the pulse duration is chosen to investigate the most interesting case where the typical el.-ph. scattering time is of the order of the pulse width. This typical time has been extracted from the spectral width introduced by the el.-ph. interarction in a linear spectrum.[22] In thermodynamic equilibrium a small fraction of the carriers is found in the upper subband, hence the population in the upper subband is nonzero before and after the excitation.

(1) Resonant excitation: Figure 2 shows Rabi flops in a 10 nm wide QW with a gap energy between the subbands of 98.45 meV and a carrier density $n = 6.0 \times 10^{11}$ cm^{-2} at the temperatures $T = 300$ K and $T = 77$ K. The exciting Gaussian pulse with a pulse area of $\Theta = 4\pi$ and pulse duration of $\tau_p = 700$ fs is centered around $t = 0$ fs. The dynamics where the el.-ph. interarction has been artificially switched off (free) does not show complete Rabi flops to a 4π pulse (two oscillations), since the different curvature of the upper and lower subband the transitions result in an energy dispersion of the transition energy and not all electrons are excited resonantly.[2] Furthermore, the damping of the Rabi oscillations through the el.-ph. interarction is only moderately stronger in the non-Markovian case. This follows from a quantum kinetic memory effect of the interarction. When performing a Markov approximation onto the PDM in Eq. (5), it is assumed that the occupations $f_{ii,\mathbf{k}}$ are constant on a relative time scale $t - \tau$. This condition is not fulfilled for nonlinear optical excitation, because the occupations do change rapidly. In consequence Markovian dynamics underestimates the damping, since there is no memory of earlier times. In principle, the variation of the phenomenological damping in Eq. (5) can be used to estimate a memory time of interarction $\tau_{\mathrm{mem}} \sim (\hbar\gamma_{\mathrm{ph}})^{-10}$, by increasing the phenomenological damping the memory time of the non-Markovian dynamics is reduced. Figure 3 shows Rabi oscillations (same effective masses in both subbands) with different values of γ_{ph}. For an increasing γ_{ph} the non-Markovian Rabi flops (solid line) approach the Markovian solution (dashed line), which clearly demonstrate the memory effect on this time scale.

(2) Off-resonant excitation: Having a much larger detuning of carrier frequency and band gap than the spectral pulse width of 2 meV, we observe a temporally adiabatic following

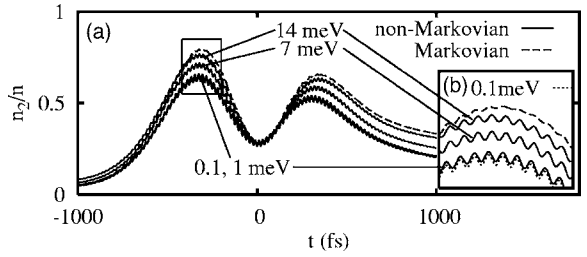

FIG. 3. (a) Relative population n_2/n of the upper subband in a 10 nm wide QW with equal subband masses that has a carrier density of $n=6.0\times10^{11}$ cm^{-2} with Markovian (dashed line) and non-Markovian, with different values of $\hbar\gamma_{\mathrm{ph}}$ (solid line), el.-ph. interarction at a lattice temperature of $T=300$ K. (b) Magnification of the box in (a), non-Markovian el.-ph. interarction with $\hbar\gamma_{\mathrm{ph}}=0.1$ meV (dotted line).

of the upper subband carrier density with respect to the exciting pulse envelope function $\tilde{E}(t)$ and a corresponding Kerr nonlinearity. This is illustrated in Fig. 4 for a detuning of 20 meV and a pulse width of 2 meV. For free carriers, the population is of the upper level clearly is proportional to $\tilde{E}^2(t)$. However, the el.-ph. interarction introduces a deviation from this ideal behavior. Here, after the carrier population of the upper subband has reached a maximum, the decay is slower and does not follow the pulse shape. This nonadiabatic behavior is caused by el.-ph. induced dephasing which typically generates a finite incoherent population after the pulse.[2] This incoherent population decays slower in comparison to free carriers via relaxation from the upper to the lower subband. From these calculations we conclude that a pure Kerr nonlinearity is not easily designable due to the counteracting el.-ph. interarction.

(3) For many quantum cascade lasers, wide QWs with small gap energies are used corresponding to transition frequencies in the THz regime.[26] It is a widespread belief that in QWs with subband gap energies smaller than the phonon energy of optical phonons close to the Γ point, the el.-ph. interarction has no major impact on ISB transitions.[27] However, this argument relies strongly on the validity of the Markov approximation, which fully suppresses the el.-ph. interarction in this limit. The more realistic quantum kinetic Eqs. (5), however, obey the energy-time uncertainty and do not rely on microscopic energy conservation for el.-ph. collisions. Hence even below the phonon energy non-Markovian el.-ph. interarction has an impact onto ISB transitions. We illustrate this for the case of Rabi oscillations.

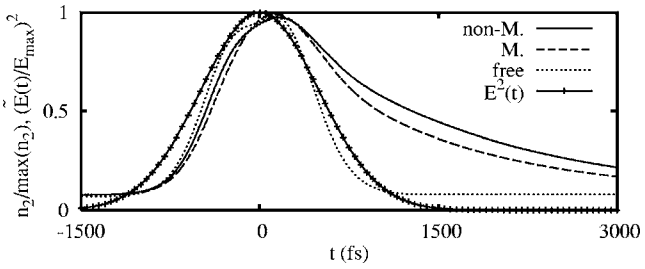

FIG. 4. Relative population of the upper subband normalized to the maximum and averaged over 50 fs for a detuning of 20 meV, with non-Markovian (solid line) and Markovian (dashed line) el.-ph. interarction at a lattice temperature $T=300$ K, as well as free carriers (dotted line) and $\tilde{E}(t)^2$ (line with dots).

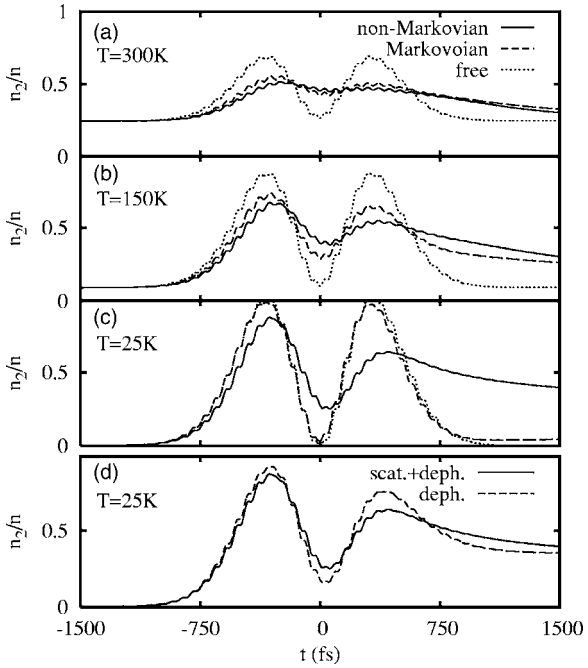

FIG. 5. Relative population n_2/n of the upper subband in a 20 nm wide QW (el. density of $n=2.0\times10^{10}$ cm^{-2}) with non-Markovian el.-ph. interarction(solid line), Markovian of (a) 300 K, (b) 150 K, (c) 25 K. (d) 25 K, and non-Markovian el.-ph. interarction with scattering and dephasing (solid line) and dephasing only (dashed line).

Figure 5 shows Rabi flops in a 20 nm wide quantum well that has a subband gap energy of 30.51 meV (i.e., below the phonon energy of 36 meV) and a carrier density of $n=2.0\times10^{10}$ cm^{-2}. For such a QW nonparabolicity effects of the band structure are less dominant, hence the effective subband masses are almost equal and the different dispersion has nearly no effect on the Rabi oscillations of the noninteracting system (dashed). It can be recognized that for high temperatures [Figs. 5(a) and 5(b)], the Markov approximation remains a valid approach, however, at 25 K [Fig. 5(c)] lattice temperature the Markovian approximation resembles the Rabi oscillations of free carriers, whereas the non-Markovian approach exhibits a considerable damping of the oscillations. At 25 K the charge distribution is centered close to the Γ point and any scattering event violates energy conservation. This is illustrated in Fig. 6 which shows the initial Fermi distributions in the lower subband at 25 K and 300 K. With increasing temperature the electron distribution function is

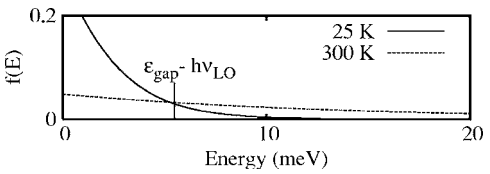

FIG. 6. Fermi-Dirac distributions for a carrier density of 2.0×10^{10} cm^{-2} at 25 K (solid line), 300 K (dashed line).

more spread out in **k** space, hence more electrons have higher kinetic energies, so that their energy is sufficient to fulfill energy conservation for the scattering and dephasing processes. Therefore, Rabi oscillations within Markov approximation are damped for sufficiently high temperatures but resemble the behavior of free charge at low temperature. Within a non-Markovian approach, however, Rabi oscillations are damped even at low temperature, resulting from nonenergy conserving processes. Damping of Rabi oscillations resulting from a violation of energy conservation has been found in quantum dots.[28] However, in this case without simultaneous energy relaxation of carriers to the lower band, these processes are therefore called pure dephasing. Pure dephasing results from virtual transitions only. In our case the dephasing is accompanied by a real transfer of carriers from the upper subband to the lower subband, Figure 5(d) shows the Rabi flops at 25 K including scattering and dephasing processes [$i=j$ and $i\neq j$ in Eq. (4)] as well as with dephasing processes only [$i\neq j$ in Eq. (4) only]. It can be recognized that both kinds of processes contribute to the damping of the Rabi oscillations.

In conclusion, we find that in the picosecond range el.-ph. interarction has an essential impact onto the damping mechanisms of nonlinear coherent phenomena in semiconductor ISB transitions. For larger QWs, with gap energies smaller than the phonon energy and a sufficiently narrow initial energy distribution of the electrons, non-Markovian dynamics is necessary to correctly describe the el.-ph. interarction.

We acknowledge financial support by the Deutsche Forschungsgemeinschaft, the "Jean Reable Stiftung," and the "Berliner Programm zur Förderung von Frauen in Forschung und Lehre." Furthermore we would like to thank Michael Woerner and Klaus Reinmann (Max Born Institute, Berlin) for helpful discussions.

*Electronic address: butscher@itp.physik.tu-berlin.de

[1] L. Allen and J. H. Eberly, *Optical Resonance and Two-Level Systems* (Dover, New York, 1987).
[2] R. Binder, S. W. Koch, M. Lindberg, N. Peyghambarian, and W. Schäfer, Phys. Rev. Lett. **65**, 899 (1990).
[3] M. Lindberg and S. W. Koch, Phys. Rev. B **38**, 3342 (1988).
[4] V. M. Axt and T. Kuhn, Rep. Prog. Phys. **67**, 433 (2004).
[5] A. A. Batista and D. Citrin, Phys. Rev. Lett. **92**, 127404 (2004).
[6] S. T. Cundiff, A. Knorr, J. Feldmann, S. W. Koch, E. O. Göbel, and H. Nickel, Phys. Rev. Lett. **73**, 1178 (1994).
[7] N. C. Nielsen, S. Linden, J. Kuhl, J. Förstner, A. Knorr, S. W. Koch, and H. Giessen, Phys. Rev. B **64**, 245202 (2001).
[8] T. H. Stievater, X. Li, D. G. Steel, D. Gammon, D. S. Kratzer, D. Park, C. Piermarocchi, and L. J. Sham, Phys. Rev. Lett. **87**, 133603 (2001).
[9] H. Kamada, H. Gotoh, J. Temmyo, T. Takagahara, and H. Ando, Phys. Rev. Lett. **87**, 246401 (2001).
[10] A. Schülzgen, R. Binder, M. E. Donovan, M. Lindberg, K. Wundke, H. M. Gibbs, G. Khitrova, and N. Peyghambarian, Phys. Rev. Lett. **82**, 2346 (1999).
[11] C. W. Luo, K. Reimann, M. Woerner, T. Elsaesser, R. Hey, and K. H. Ploog, Phys. Rev. Lett. **92**, 047402 (2004).
[12] T. Müller, W. Parz, G. Strasser, and K. Unterrainer, Phys. Rev. B **70**, 155324 (2004).
[13] Subband masses (units of m_0), 10 nm wide well: $m_1=0.071$, $m_2=0.088$, 20 nm wide well: $m_1=0.068$, $m_2=0.072$.
[14] B. Krummheuer, V. M. Axt, and T. Kuhn, Phys. Rev. B **65**, 195313 (2002).
[15] J. Förstner, K. J. Ahn, J. Danckwerts, M. Schaarschmidt, I. Waldmüller, C. Weber, and A. Knorr, Phys. Status Solidi B **234**, 155 (2002).
[16] U. Ekenberg, Phys. Rev. B **40**, 7714 (1989).
[17] L. Banyai, D. B. Trar Thoai, E. Reitsamer, H. Haug, D. Steinbach, M. U. Wehner, M. Wegener, T. Marschner, and W. Stolz, Phys. Rev. Lett. **75**, 2188 (1995).
[18] E. Binder, J. Schilp, and T. Kuhn, Phys. Status Solidi B **206**, 227 (1998).
[19] Z. Wang, K. Reimann, M. Woerner, T. Elsaesser, D. Hofstetter, J. Hwang, W. J. Schaff, and L. F. Eastman, Phys. Rev. Lett. **94**, 037403 (2005).
[20] I. Waldmüller, J. Förstner, S.-C. Lee, A. Knorr, M. Woerner, K. Reimann, R. A. Kaindl, T. Elsaesser, R. Hey, and K. H. Ploog, Phys. Rev. B **69**, 205307 (2004).
[21] J. Li and C. Z. Ning, Phys. Rev. B **70**, 125309 (2004).
[22] S. Butscher, J. Förstner, I. Waldmüller, and A. Knorr, Phys. Status Solidi B **241**, R49 (2004).
[23] R. Zimmermann, Phys. Status Solidi B **159**, 317 (1990).
[24] T. Kuhn, in *Theory of Transport Properties of Semiconductor Nanostructures*, edited by E. Schöll (Chapman & Hall, London, 1998), Chap. 6, p. 173.
[25] I. Waldmüller, J. Förstner, and A. Knorr, in *Self-Consistent Projection Operator Theory of Intersubband Absorbance in Semiconductor Quantum Wells*, edited by K. Morawetz (Springer, New York, 2004).
[26] M. F. Pereira, S.-C. Lee, and A. Wacker, Phys. Rev. B **69**, 205310 (2004).
[27] P. Harrison, *Quantum Wells, Wires and Dots* (Wiley, New York, 1999), Chap. 8.5.
[28] J. Förstner, C. Weber, J. Danckwerts, and A. Knorr, Phys. Rev. Lett. **91**, 127401 (2003).